JOURNAL OF AGRICULTURAL AND FOOD CHEMISTRY

ARTICLE

pubs.acs.org/JAFC

Hibiscus sabdariffa Polyphenolic Extract Inhibits Hyperglycemia, Hyperlipidemia, and Glycation-Oxidative Stress while Improving Insulin Resistance

Chiung-Huei Peng,[†] Charng-Cherng Chyau,[‡] Kuei-Chuan Chan,[§,∥] Tsung-Hsien Chan,[⊥] Chau-Jong Wang,[*,⊥,#] and Chien-Ning Huang[*,§,#,▽]

[†]Division of Basic Medical Science and [‡]Institute of Biotechnology, Hungkuang University, Number 34, Chung Chie Road, Shalu County, Taichung 433, Taiwan

[§]Department of Internal Medicine, Chung-Shan Medical University Hospital, Number 110, Section 1, Chien-Kuo North Road, Taichung 402, Taiwan

[∥]School of Medicine, [⊥]Institute of Biochemistry and Biotechnology, and [▽]Institute of Medicine, Chung-Shan Medical University, Number 110, Section 1, Chien-Kuo North Road, Taichung 402, Taiwan

ABSTRACT: *H. sabdariffa* polyphenolic extract (HPE) was demonstrated to inhibit high glucose-stimulated cellular changes. In this study, we analyzed the composition of HPE and used a type 2 diabetic rat model to test its protective effect. At least 18 phenolic compounds were found in HPE. Treatment with HPE reduced hyperglycemia and hyperinsulinemia, especially at the dose of 200 mg/kg. HPE decreased serum triacylglycerol, cholesterol, and the ratio of low density lipoprotein/high density lipoprotein (LDL/HDL). Diabetes promoted plasma advanced glycation end product (AGE) formation and lipid peroxidation, while HPE significantly reduced these elevations. Immunohistological observation revealed that HPE inhibited the expression of connective tissue growth factor (CTGF) and receptor of AGE (RAGE), which was increased in type 2 diabetic aortic regions. Furthermore, HPE recovered the weight loss found in type 2 diabetic rats. In conclusion, we demonstrated the anti-insulin resistance properties of HPE and its effect on hypoglycemia, hypolipidemia, and antioxidation. HPE has the potential to be an adjuvant for diabetic therapy.

KEYWORDS: *H. sabdariffa* polyphenolic extract, type 2 diabetes, insulin resistance, advanced glycation end product

INTRODUCTION

Diabetes mellitus is a highly prevalent disease worldwide with a consistent increase in mortality, and accompanying vascular complications including coronary heart disease, nephropathy and neurodegeneration. Diabetes-associated metabolic syndrome is manifested as hyperglycemia, high triacylglycerol (TG), and low high density lipoprotein (HDL) dyslipidemia. For type 2 diabetes, which is characterized as insulin-resistant and often associated with overproduction of free fatty acid (FFA), obesity is suggested to be a critical morbidity factor in the pathogenesis.[1]

Hyperglycemia, one of the pathogenic factors involved in diabetic injuries, promotes the formation of advanced glycation end product (AGE).[2] Interacting with its specific receptor (RAGE), AGE, inducing the generation of reactive oxygen species (ROS) and mediating its action via oxidative stress, was demonstrated to play a key role in atherosclerotic plaque formation in a diabetic rat model.[3] Although ROS are generated under physiological conditions, the overload oxidative burden leads to pathological consequences, including damage to protein, lipid and DNA. In addition, the cysteine-rich secreted peptide connective tissue growth factor (CTGF) was also reported to be involved in diabetic vasculopathy and nephropathy.[4]

Hibiscus sabdariffa (*H. sabdariffa*) L., a native tropical plant, is widely cultivated in Eastern Taiwan and commonly used as a local soft drink against inflammation, hypertension, and liver disorders. Previous studies showed that *H. sabdariffa* possessed multieffects, including antioxidation and antihyperlipidemia, which inhibited low density lipoprotein (LDL) oxidation and lowered serum TG, cholesterol, and LDL cholesterol in animal experiments.[5−7] Compared with the crude extract, the polyphenolic extract of *H. sabdariffa* (HPE) was more potent in decreasing serum LDL cholesterol and increasing HDL cholesterol, and more effective in lowering the hepatic lipid content and enhancing LDL uptake in hepatocytes.[8]

Recently, HPE was demonstrated to inhibit high glucose-stimulated proliferation and migration of vascular smooth muscle cells via regulating CTGF, AGE, and the downstream signals, implying the potential of HPE to protect against diabetic vasculopathy.[9] In vivo experiments showed that HPE was beneficial in improving the serum lipid profile, in preventing renal damage, and also in antioxidation in STZ-induced type 1 diabetic rats.[10] However, type 2 diabetes accompanied with obesity is indeed the most prevalent form of diabetes. Based on this, in the present study, we modified a type 2 diabetes model which had been used previously.[11] We analyzed the composition of HPE and observed whether HPE could effect changes in serum insulin, glucose, lipid profile, oxidative stress, and the

Received: June 4, 2011
Accepted: August 29, 2011
Revised: August 28, 2011
Published: August 29, 2011

characteristic biomarkers of AGE/RAGE and CTGF, hence preventing or reducing diabetic injury.

MATERIALS AND METHODS

Preparation of HPE. Five grams of dried ground *H. sabdariffa* L. calyx was extracted with 50 mL of an HPLC-grade methanol and stirred in a 60 °C water bath for 30 min. The extract was filtered through a Whatman No. 4 filter paper, and the residue was extracted twice more with the same procedure as the above. The extracts were pooled and evaporated to dryness (at ≤5 °C) using a vacuum (20 mbar). The residue (2.27 ± 0.13 g) was solubilized in 10 mL of deionized water (pH 2.3, with 0.1 N HCl), and then the aqueous solution was partitioned successively with *n*-hexane (3 × 10 mL) and ethyl acetate (3 × 10 mL). Using a rotary evaporator (Buchi, Switzerland), the ethyl acetate soluble fraction was evaporated to dryness using a vacuum (about 0.44 ± 0.06 g was yielded). The dried crude extract was stored at −20 °C for further experiments; it was redissolved in methanol for chemical analysis or in water for animal feeding.

Chemical Analysis of HPE. *Total Phenolic and Flavonoid Contents.* The total phenolic contents were measured by photometric assay using a Folin−Ciocalteu reagent.[12] 2.5 mL of water-diluted Folin−Ciocalteu reagent (50%, Fluka, Buchs, Switzerland) was added to 0.5 mL of each sample. The mixture was incubated for 2 min at room temperature, and 2 mL of sodium carbonate (0.75 g/mL) was added. The mixture was incubated for 15 min at 50 °C and finally cooled in a water−ice bath. The specific absorbance at 760 nm was immediately measured with a spectrophotometer (Thermo Biomate 5, Thermo Electron Corporation, San Jose, CA, USA). Gallic acid (GA) was used as a standard phenolic compound for the calibration curve ($y = 0.7758x + 0.0582$, $R^2 = 0.9982$). Total phenolic content was expressed as mg of gallic acid equivalents per gram of dry weight of plant (mg GA/g DW).

Total flavonoid contents were determined by the following procedures.[13] A volume of 0.5 mL of extract was placed in a 5 mL volumetric flask. Five minutes after adding 2.5 mL of distilled water and 0.15 mL of $NaNO_2$ (5%) to the flask, 0.3 mL of $AlCl_3$ (10%) solution was added. After 6 min, 1 mL of 1 M NaOH was added and the total was brought up to 5 mL with distilled water. The solution was mixed well again, and the absorbance of the final mixture was measured against a blank at 510 nm (Thermo Biomate 5). Quercetin (Qr) was used for the calibration curve ($y = 0.8551x + 0.0586$, $R^2 = 0.9989$). The total flavonoid contents of the extract were expressed as mg of quercetin (Qr) equivalents per gram of dry weight of plant (mg Qr/g DW).

HPLC Analysis. Chromatography was performed on a Finnigan Surveyor module separation system and a photodiode-array (PDA) detector together with a quaternary pump (Thermo Electron Co., MA, USA). The separation was performed using a Phenomenex Luna C18(2) analytical column (150 mm × 2.0 mm, 3 μm particle size) with a precolumn (SecurityGuard C18(ODS) 4 mm × 3.0 mm i.d., Phenomenex Inc., Torrance, CA, USA). Gradient elution using solvent A (10 mM ammonium acetate in water, pH4.0 with formic acid, FA) and solvent B (acetonitrile/methanol = 4/3, v/v, containing 0.1% FA) as the mobile phase at a flow rate of 0.2 mL/min was applied. The gradient conditions were as follows: 0−25 min, linear from 10% to 20% B; 25−50 min, linear from 20 to 50% B; 50−60 min, linear from 50 to 95% B; 60−65 min held at 95% B, then returned to 10% B in 5 min. The injection volume was 20 μL. The absorption spectra of eluted compounds were scanned within 190 to 600 nm using the in-line PDA detector monitored at 325 nm for polyphenolic compounds and 518 nm for anthocyanins, respectively.

LC−MS/MS Analysis. The phenolics and anthocyanins that were eluted and separated were further identified with a Finnigan LCQ Advantage MAX ion trap mass spectrometer. The system was operated in electrospray ionization (ESI) with positive and negative ionization modes. The typical operating parameters in the negative ionization mode were as follows: ion spray voltage, 3.5 kV; capillary voltage, −15 V; tube lens offset, −20 V; ion transfer capillary temperature, 300 °C; nitrogen sheath gas, 40; and auxiliary gas, 5 (arbitrary units). In the positive ionization analyses, ion spray voltage (4.0 kV), capillary voltage (30 V), tube lens offset (40 V), and ion transfer capillary temperature (220 °C) were used. Mass spectra were acquired with a scan range of 150−800 amu, with 5 microscans and a maximum ion injection time of 200 ms. The SIM analysis was a narrow scan event that monitored the m/z value of the selected ion, in a range of 1.0 Th centered on the peak for the molecular ion; this was used in the analysis of molecular ions of the phenolic compounds and anthocyanins. For MS/MS analysis, helium collision gas was introduced in accordance with the manufacturer's recommendations. The MS/MS fragment spectra were produced using normalized collision energies between 25% and 40% with wideband activation "off". All the data were processed with the Xcalibur 2.0 data system (Thermo Electron Co.).

Table 1. Ingredients of Experimental Animal Diets[a]

ingredient/group	C (%)	H (%)
casein	20.0	20.0
sucrose	6	6
corn starch	51.8	37.8
corn oil	12.0[b]	25.9[b]
cholesterol		0.1
mineral premix[c]	4	4
vitamin premix[d]	1	1
choline	0.2	0.2
cellulose	5	5
total	100	100

[a] Based on AIN-76 formula (AIN, 1997). [b] Amounts of corn oil were expressed in wt %. C: control diet containing corn oil 12%. H: high fat diet containing corn oil 25.9%. [c] Mineral premix: $CaHPO_4 \cdot 2H_2O$, NaCl, $K_3C_6H_5O_7$, K_2SO_4, MgO_3, MnO_3, Fe-citrate, $ZnCO_3$, $CuCO_3$, KI, $NaSeO_3$, $K_2SO_4 \cdot Cr_2(SO_4)_3 \cdot 24H_2O$. [d] Vitamin premix: thiamine hydrochloride, pyridoxine hydrochloride, riboflavin, nicotinic acid, vitamin B12, retinyl palmitate, vitamin D3, vitamin E, vitamin K.

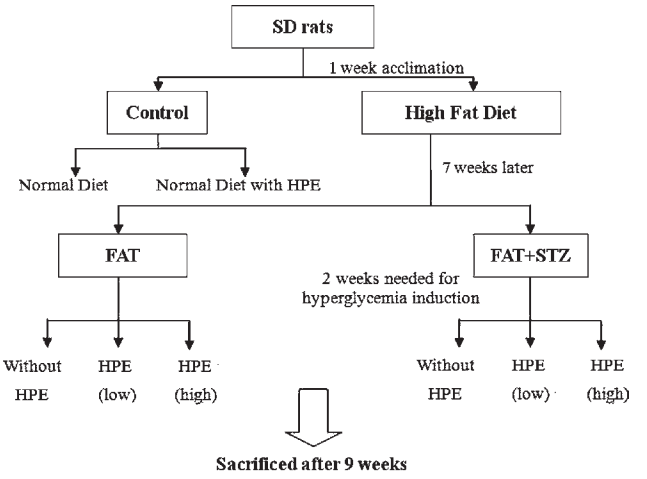

Figure 1. Flowchart of animal experiment.

Animal Experiments. *Animals and Diets.* The animal experimental project was approved by the Animal Model Experimental Ethics Committee of Chung-Shan Medical University and was in accordance with the 1972 Helsinki Declaration. Briefly, male Sprague−Dawley (SD)

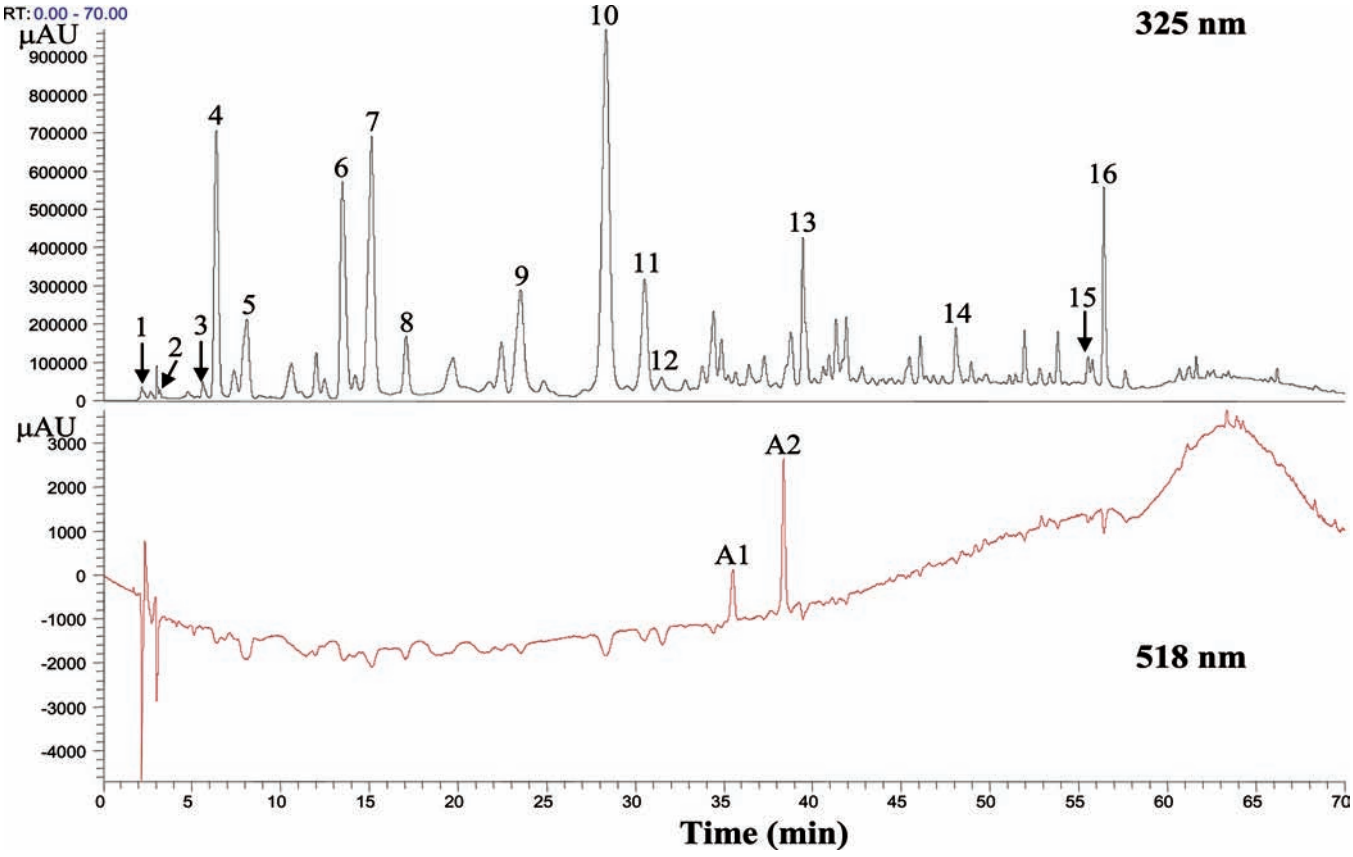

Figure 2. HPLC/UV chromatograms of HPE. Compositions of the extract were detected at 325 and 518 nm respectively. Peak numbers refer to Table 2.

Table 2. Retention Time, UV−Vis, and Mass Spectral Characteristics for the Phenolics Identified in HPEP[a]

peak	compound	t_R (min)	X (nm)	$[M + H]^+$	MS^2	$[M - H]^-$	MS^2
1	hibiscus acid[b]	2.3	235, 219 sh			189	127, 83
2	hibiscus acid 6-methyl ester[b]	3.1	234			203	141, 185, 127
3	gallic acid[c]	5.3	271, 225			169	125
4	unidentified[d]	6.3	339, 238			493	
5	5-hydroxymethylfurfural[c]	8.1	285, 234	127	109, 81		
6	protocatechuic acid[c]	11.3	260, 227, 295			153	109
7	5-caffeoylquinic acid[b]	15.1	328, 300 sh, 247, 226			353	191, 179, 135
8	feruloyl derivative[d]	17.1	286, 338, 226 sh			297	
9	chlorogenic acid[c]	23.5	329, 297 sh, 247, 227			353	191, 179, 135
10	4-caffeoylquinic acid[b]	28.3	329, 298 sh, 244			353	179, 173, 191
11	caffeic acid[c]	30.5	324, 235, 296 sh			179	135
12	galloyl ester[d]	31.5	277, 231			447	
13	feruloyl quinic derivative[d]	39.5	330, 297 sh, 242			367	161, 135, 193
14	kaempferol-3-glucoside[b]	48.1	321, 237			447	285
15	quercetin derivative[d]	55.5	374, 257, 230 sh			593	301
16	tiliroside[b]	56.4	317, 269, 236			593	285, 447, 307
Al	delphinidin-3-sambubioside[b]	35.5	526, 330, 238	597	303, 465		
A2	cyanidin-3-sambubioside[b]	38.4	283, 235, 519	581	287		

[a] Tiliroside: kaempferol-3-*O*-β-D-(6″-*E*-*p*-coumaroyl)-glucopyranoside. Characteristically, the anthocyanins exhibit maxima of 280−300 nm and 500−540 nm. MS and MS^2 analysis in the positive and negative ion modes were conducted owing to their complementary results. The total phenolic and flavonoid compounds were estimated as 58.80 ± 1.34 mg and 13.57 ± 0.65 mg per gram of dried flower, respectively. [b] Compounds were tentatively identified according to mass spectra and the matched data from the literature or the citation. [c] The identification was confirmed further by authentic compound. [d] Compounds were limitedly identified from mass spectra and UV−visible absorbance spectra.

dx.doi.org/10.1021/jf2022379 |*J. Agric. Food Chem.* 2011, 59, 9901–9909

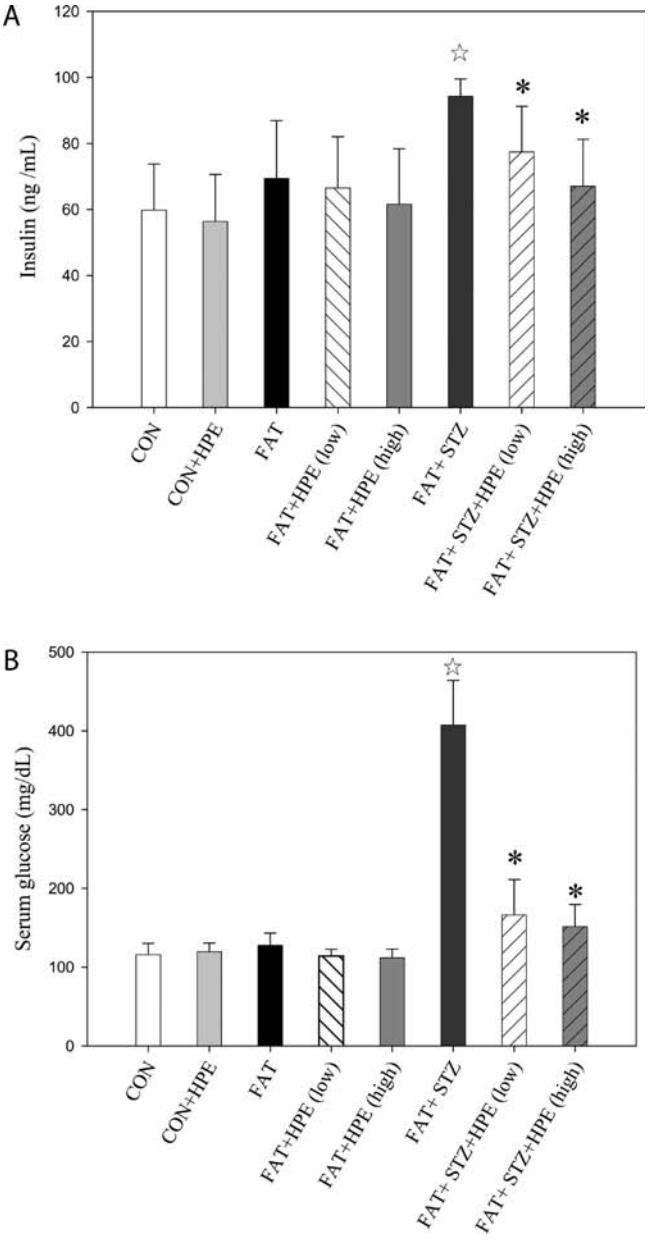

Figure 3. Effect of HPE on blood glucose and insulin levels. Serum from the experimental animals was collected, and the glucose and insulin concentrations were analyzed. (A) Serum levels of glucose. (B) Serum levels of insulin. Data are presented as mean ± SD ($n = 8$ per group) and analyzed with ANOVA and unpaired t test. (*) $p < 0.05$ compared with the FAT + STZ group. (☆) $p < 0.05$ compared with the control.

rats (weight 250 ± 20 g, age 7 weeks) were obtained from LuxBiotech Co., Taiwan. The rats, 8 for each group and 4 in each cage, were acclimated and fed a basic chow consisting of 12% fat for the first week before experimentation. The animal room was conditioned at a 12 h light/dark cycle, 25 ± 1 °C, and 55 ± 5% relative humidity. All animals had free access to food and water.

Type 2 Diabetic Animal Model. A modification of the Peng et al. method[11] was used to induce type 2 diabetes in the rats. Briefly, the rats were divided into the following groups: control (normal diet), HPE (normal diet with 200 mg/kg HPE added), FAT (high fat diet), FAT + HPE (low) (high fat diet with 100 mg/kg HPE added), FAT + HPE (high) (high fat diet with 200 mg/kg HPE added), FAT + STZ, FAT + STZ + HPE (low), and FAT + STZ + HPE (high) (Figure 1). Using the formulation described in AIN-76, the animal diets were prepared according to the formula listed in Table 1. After 7 weeks, when the average body weight attained 425 ± 15 g, the high fat diet fed rats were divided into FAT and FAT + STZ groups. The latter were injected intraperitoneally (ip) with a dose of STZ 35 mg/kgbw. To serve as a blank, the other groups received only the same amount of 0.1 M citric acid buffer (pH 4.5). About 2 weeks later, when the hyperglycemic status was confirmed, rats were tube-fed with or without different doses of HPE. The same amount of normal saline was used to serve as the blank.

Serum Biochemical Assays. All animals were fasted overnight for 8−10 h before the experiments were conducted. The serum sample was collected using EDTA tubes and centrifuged at 3,000 rpm for 10 min at 4 °C. Concentrations of TG, total cholesterol, LDL cholesterol, HDL cholesterol, and FFA were measured by enzymatic colorimetric methods using commercial kits (Randox Laboratories Ltd., Antrim, U.K.). Plasma glucose was measured by enzymatic colorimetric methods using an automatic analyzer (Olympus AU2700, Olympus Co., Tokyo, Japan). Plasma insulin concentration was determined by ELISA using a rat-insulin enzyme immunoassay kit (A05105-96 Wells, SPI-BIO).

Advanced Glycation End Products. AGE was measured using the OxiSelect Advanced Glycation End Product ELISA Kit (Cell Biolabs, CA). Briefly, 100 μL of serum serum (diluted to 10 μL/mL in 1× PBS) or AGE-BSA prepared standards was added to a 96-well plate and stored at 4 °C overnight. Each well was washed with 1× PBS and incubated with assay diluent for 1−2 h at room temperature. Rinsed with wash buffer, anti-AGE antibody was added to each well, incubated for 1 h at room temperature, and then reacted with secondary antibody−HRP conjugate. Substrate solution was added followed by incubation at room temperature for 30 min. Finally, the enzyme reaction was stopped by adding stop solution. Each sample and AGE-BSA standard was assayed in triplicate. AGE formations were measured at 450 nm using a Microplate spectrophotometer (Molecular Device/Spec384). The reduced BSA standard was used as an absorbance blank.

Thiobarbituric Acid Reaction Substances (TBARS). Lipid peroxidation was determined by measuring the TBARS. First, 0.04 mL of serum was mixed with 0.16 mL of dd H_2O, and the protein content was determined with a Bio-Rad protein assay reagent using bovine serum albumin as the standard. The calibration curve ranged from 0 to 400 μg/mL ($r^2 = 0.9913$). 0.3 mL of serum was then added with 0.2 mL of TBA (1% thiobarbituric acid in 0.3% of NaOH) to react for 40 min at 95 °C in the dark. After the reaction, samples were analyzed in a Hitachi F2000 spectrophotofluorimeter with excitation at 532 nm and emission at 600 nm. The calibration curve was prepared with malondialdehyde (MDA) standards of 0−50 nmol ($r^2 = 0.9927$). The concentrations of TBARs were expressed as equivalents of MDA represented as μM/mg protein.

Immunohistochemistry. At the end of the experiment, the rats were sacrificed by decapitation. Thereafter, the serum, aorta arch, and organ samples were collected for further investigations. All tissues were fixed in 4% paraformaldehyde overnight and embedded in paraffin by routine procedure. Consecutive 4 μm paraffin sections were made. The primary antibodies of RAGE and CTGF were obtained from Biologo (Kronshagen, Germany) and SantaCruz Biotechnology (Santa Cruz, CA), respectively. Immunostain was completed using the UltraSensitive S-P kit (Maxim Co., streptavidin peroxidase method).

Statistical Analysis. In the animal experiments, the statistical software SPSS v.12.0 was used to analyze the data. One-way ANOVA was performed to compare the differences among the CON, CON + HPE, FAT, and FAT + STZ groups ($P < 0.05$), while the TUKEY method was used for post hoc testing. In addition, we used the t test to analyze the effect of HPE treatment between the FAT and FAT + HPE; FAT + STZ and FAT + STZ + HPE groups.

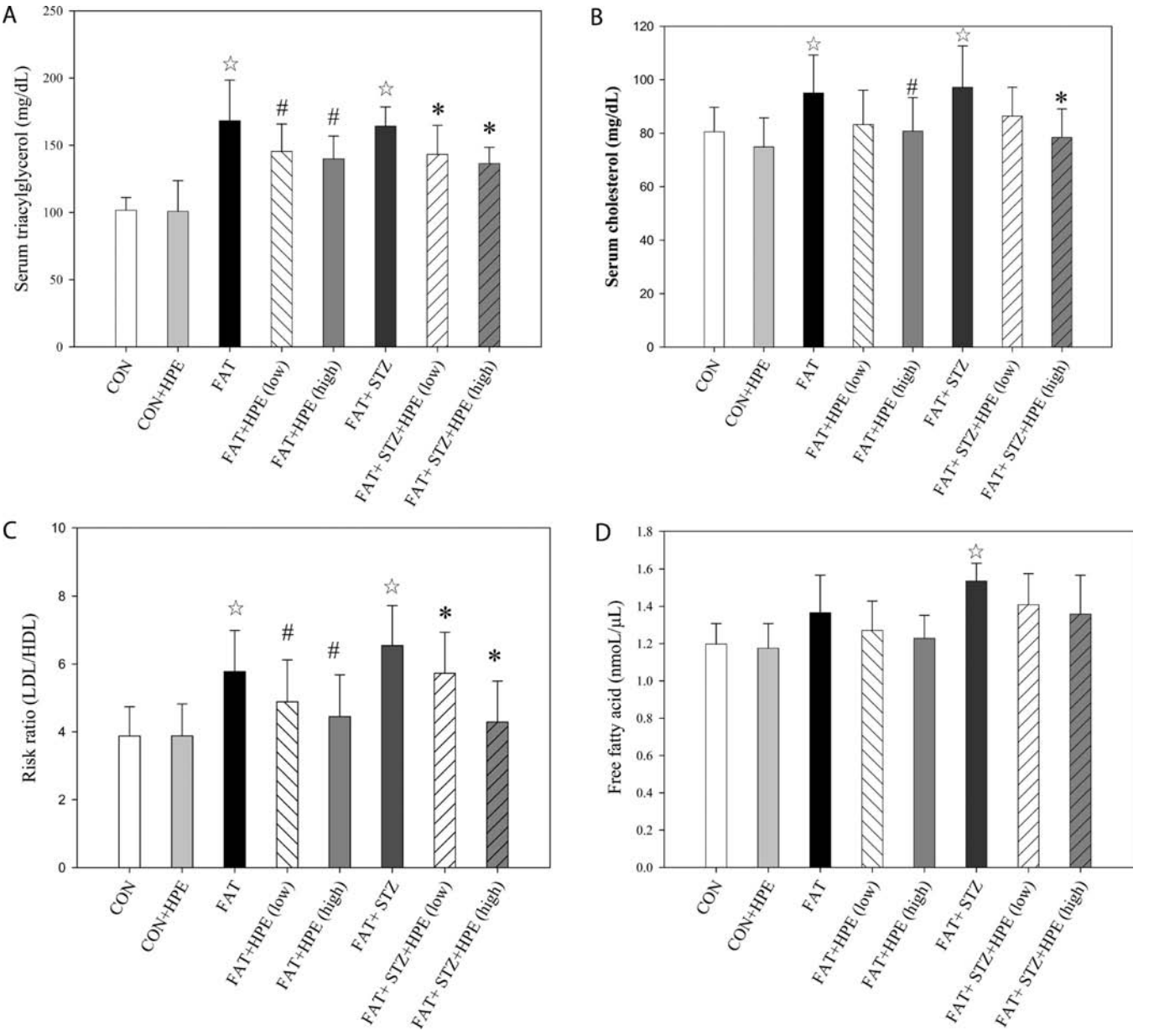

Figure 4. Effect of HPE on serum lipid levels. Serum from the experimental animals was collected, and the lipid biomarkers were analyzed. (A) Serum levels of TG. (B) Serum levels of cholesterol. (C) Serum levels of LDL/HDL. (D) Serum levels of FFA. Data are presented as mean ± SD (n = 8 per group) and analyzed with ANOVA and unpaired t test. (#) $p < 0.05$ compared with the FAT group. (*) $p < 0.05$ compared with the FAT + STZ group. (☆) $p < 0.05$ compared with the control.

RESULTS

HPE Composition. The total phenolic and flavonoid compounds contained in *H. sabdariffa* L. were estimated as 58.80 ± 1.34 mg and 13.57 ± 0.65 mg per gram of dried flower, respectively. The identification of phenolic compounds and hibiscus acid-related compounds was carried out comparing their retention times and mass spectra, as provided by ESI-MS and ESI-MS/MS. The identified composition of HPE is shown in Figure 2 and Table 2.

HPE Exhibited a Hypoglycemic Effect. Figure 3A shows that neither HPE nor FAT per se affected the serum glucose level, whereas FAT + STZ elevated blood glucose about 3.5-fold, compared with the control. One hundred mg/kg and 200 mg/kg HPE significantly reduced the diabetic high glucose by about 60% and 65%, respectively, indicating that HPE possessed a hypoglycemic ability in vivo.

HPE Shown as Anti-Insulin-Resistant. Serum insulin levels were measured to investigate whether high glucose status was accompanied with hyperinsulinemia, the most characteristic feature of type 2 diabetes. It was noted that FAT seemed to elevate the serum insulin level slightly. FAT + STZ was demonstrated to increase the serum insulin 1.6-fold as compared with the control, while HPE dose-dependently lowered the insulin level (Figure 3B). At the dose of 200 mg/kg, HPE was almost able to ameliorate the hyperinsulinemia induced by FAT + STZ, indicating the anti-insulin-resistant potential of HPE.

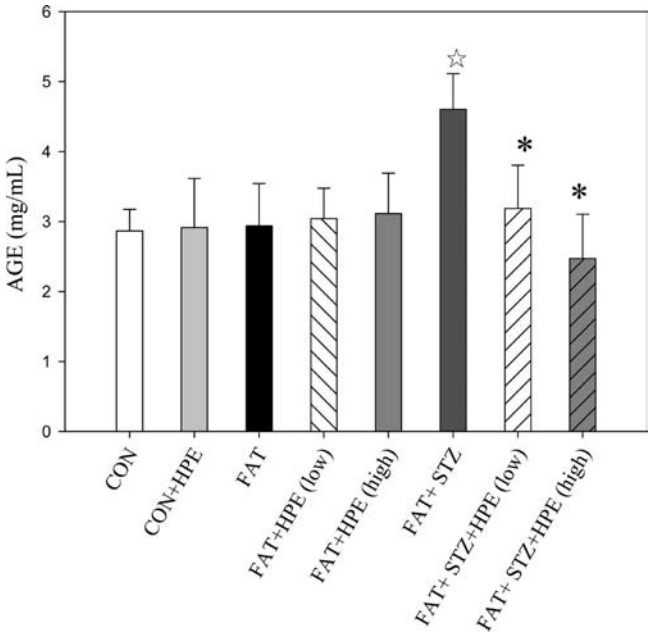

Figure 5. Effect of HPE on serum AGE. Serum was collected and analyzed with an AGE-immunoassay kit. Data are presented as mean ± SD ($n = 8$ per group) and analyzed with ANOVA and unpaired t test. (#) $p < 0.05$ compared with the FAT group. (*) $p < 0.05$ compared with the FAT + STZ group. (☆) $p < 0.05$ compared with the control.

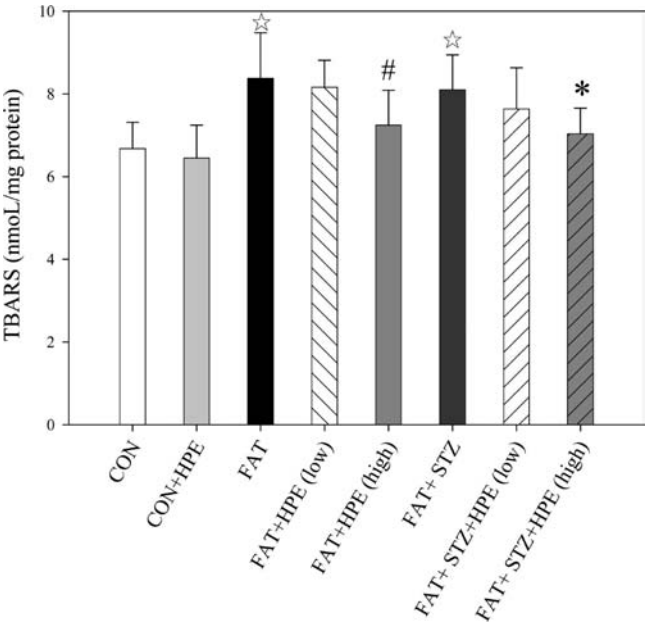

Figure 6. Effect of HPE on serum lipid peroxidation. Serum was collected and analyzed with TBARS. Data were presented as mean ± SD ($n = 8$ per group) and analyzed with ANOVA and unpaired t test. (#) $p < 0.05$ compared with the FAT group. (*) $p < 0.05$ compared with the FAT + STZ group. (☆) $p < 0.05$ compared with the control.

HPE Showed Hypolipidemic Effects. Serum TG and cholesterol were elevated in both the FAT and FAT + STZ groups. Treatment with HPE reduced the plasma level of TG and cholesterol, especially at the dose of 200 mg/kg (Figures 4A and 4B). The increase of LDL/HDL (which is recognized as the risk ratio of atherogenesis) was 53% and 75% in the FAT and FAT + STZ groups, respectively, while HPE decreased the ratio of LDL/HDL induced by obesity and insulin resistance (Figure 4C).

Although the serum FFA was not significantly altered, it was still elevated about 13% and 28% in the FAT and FAT + STZ groups, respectively. HPE was also shown to reduce the serum FFA (Figure 4D).

HPE Inhibited AGE Formation. The diabetic status has the potential to promote the Millard reaction and the generation of AGE. Figure 5 shows that the amount of AGE reached 1.7-fold in the FAT + STZ group, compared with the control. Treatment with 100 mg/kg HPE significantly reduced AGE by 32%. At the higher dose of 200 mg/kg, HPE lowered AGE generation even more, compared with the control (Figure 5).

HPE Possessed an Antioxidative Ability. TBARS analysis revealed that obesity and type 2 diabetes enhanced lipid peroxidation, while HPE, especially at a high dose, effectively inhibited peroxidation and exhibited good antioxidative ability (Figure 6).

HPE Reduced the Vascular Expression of RAGE and CTGF. Immunohistochemistry analysis revealed that aortic RAGE increased in the type 2 diabetic status, while HPE, especially at the high dose of 200 mg/kg, effectively suppressed the formation of RAGE (Figures 7A−7C, brown stain). Since RAGE mediated vascular cellular changes through CTGF and the downstream signals, we investigated whether CTGF expression would be altered in vivo.

The brown-stained region of Figures 7D−7F shows that CTGF increased in type 2 diabetic rats, and that 200 mg/kg of HPE inhibited the expression of CTGF. These results implicated that HPE could be protective in diabetic vasculopathy via reducing the pathogenic markers of RAGE and CTGF.

HPE Possessed a Weight-Balancing Ability. At 10 weeks, the weight of the type 2 diabetic rats reached its highest level, and thereafter it declined gradually until the end of the experiment. These phenomena coincide with clinical findings among type 2 diabetic patients. However, treatment with HPE impeded the decrease in weight, and the lost weight was recovered after 14 weeks (Figure 8).

DISCUSSION

In this study, using a type 2 diabetic model with the characteristics of high glucose and hyperinsulinemia, we demonstrated the effect of HPE in lowering blood glucose and ameliorating insulin resistance. HPE is hypolipidemic and reduces the parameters elevated in obesity and the diabetic status, such as serum TG, cholesterol, and the risk ratio of LDL/HDL. In addition to its antioxidative effect, HPE suppressed the formation of RAGE and CTGF, which could be pathogenic biomarkers in type 2 diabetes-associated vasculopathy.

High glucose has been shown to trigger CTGF expression via TGF-1 and protein kinase C, and thus mediated matrix production.[14] In our previous report, the proliferation signal of high glucose-treated vascular smooth muscle cells was mediated via CTGF/RAGE,[9] while in the literature, AGE significantly stimulated cell proliferation and CTGF expression in cardiac fibroblasts.[15] These previous reports demonstrated that AGE/RAGE acted as a critical mediator in diabetic cellular changes.

We observed an elevation of AGE in both the serum and vascular tissue of the diabetic animals, accompanied with an increase in lipid peroxidation analyzed with TBARS. These results suggested that oxidative stress could be involved in the

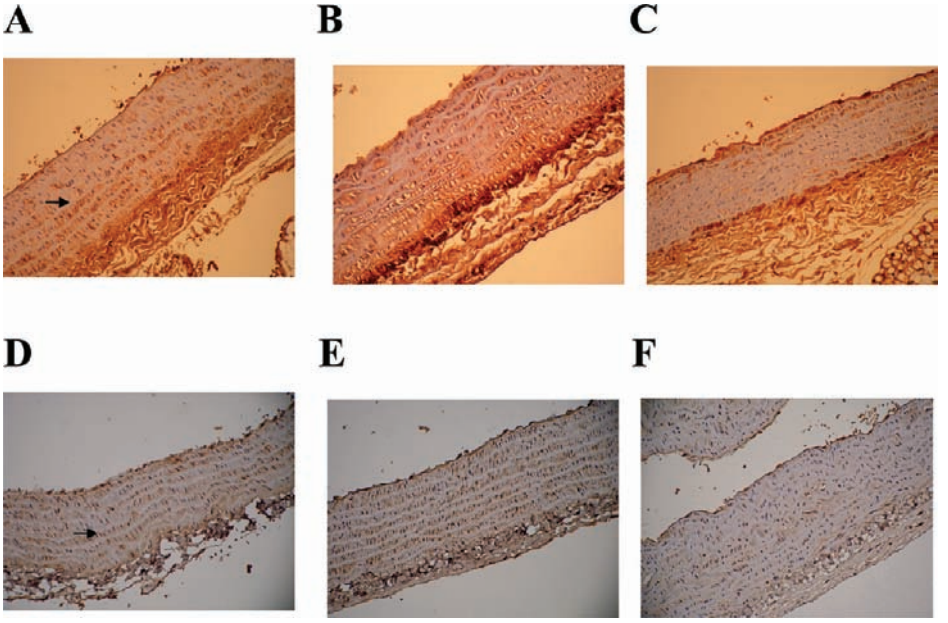

Figure 7. Effect of HPE on expression of RAGE and CTGF. (A−C) immunohistochemistry examination (200×) of RAGE in rat aorta: (A) control, (B), diabetic, and (C) 200 mg/kg of HPE-treated diabetic groups. (D−E) Immunohistochemistry examination (200×) of CTGF in rat aorta: (A) control, (B) diabetic, and (C) 200 mg/kg of HPE-treated diabetic groups. The brown staining of RAGE and CTGF is indicated by arrows in A and D, respectively.

pathogenesis of diabetic injury. In previous reports, high glucose and AGE induced oxidative stress, which could impair pancreatic beta-cell function and the modification of LDL.[16,17] AGE modification impaired receptor-mediated clearance, and might contribute to the elevation of LDL in diabetic patients. AGE increased ROS formation and activated the mitogen-activated protein kinase system, and thus mediated diabetic vasculopathy.[18] A recent report demonstrated that RAGE-induced phosphatidylinositol-3 kinase activity was associated with ROS generation, caspase-3 activation, and nuclear DNA degradation in dorsal root ganglia neurons. Hence, blocking AGE/RAGE signals or preventing oxidative stress should be a focus in the therapy of diabetic injury-prone tissues.[19]

Many reports have indicated the correlation between obesity and oxidative stress. Obesity is associated with the proinflammatory state, in which the impairments of oxidative stress and the antioxidant mechanism can be involved. Disorders of mitochondrial electron transports and overgeneration of ROS have been implicated in obesity and type 2 diabetes.[20] In adipose tissue, macrophage infiltration and the hypoxic status are enhanced, thereby generating oxidative stress. It has been proposed that proton imbalance, which inhibits mitochondrial energy production, is associated with the generation of ROS.[21] It has been suggested that high cytosolic TG increased concentrations of long-chain acyl-CoA esters, and thus inhibited adenine nucleotide translocators and caused intramitochondrial ADP deficiency, a potent stimulator of free radical production. Tissues with poor scavenging capacity or high energy demand, such as beta-cells, are likely to be more susceptible.[22]

Our data showed that serum FFA was elevated in the obese and diabetic groups, although not to a statistically significant level. The increase in serum FFA is considered to be critical to obesity and its related metabolic complications, such as dyslipidemia and insulin resistance. The total FFA rate of appearance (R_a) was reported to increase linearly with an increase in fat

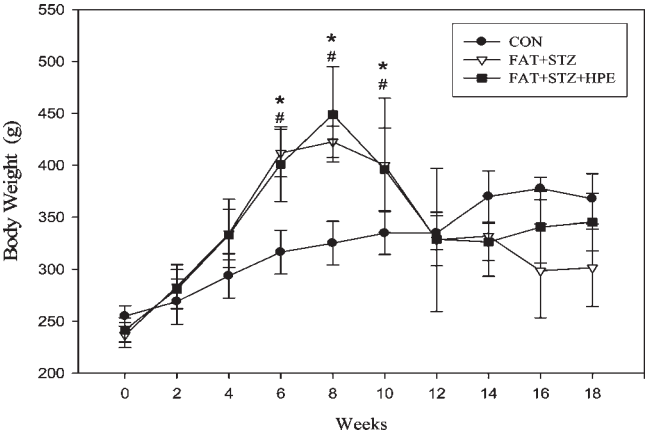

Figure 8. Effect of HPE on body weight change. Rats were fed different diets and weighed every week, until the end of the experiment. Data were presented as mean ± SD (n = 8 per group) and analyzed with ANOVA and unpaired t test. (*) $p < 0.05$ for the diabetic group compared with the control. (#) $p < 0.05$ for the 200 mg/kg of HPE-treated diabetic groups compared with the control.

mass.[23] High FFA levels have been shown to modulate microvascular function, and contribute to obesity-associated hypertension and microangiopathy.[24] FFA-associated insulin resistance could be mediated by the molecular mechanism in beta cells involving GPR40 and insulin receptor substrate-1 serine kinase, which played a critical role in the development of insulin resistance, and regulated the insulin receptor signal pathway.[25]

In insulin target cells, lipid-induced insulin resistance could result from defects in glucose transport. The intracellular accumulations of diacylglycerol triggered the activation of protein kinase C and subsequent impairment of insulin signaling, and then impeded the regulation of glucose production, glycogen

synthesis, and the glycolysis pathway.[26] Palmitate was found to inhibit insulin receptor gene expression via phosphorylation of PKC (eta).[27] The insulin action is initiated from receptor-binding, autophosphorylation of receptor tyrosine kinase, and tyrosine phosphorylation of IRS. The signals transduced by IRS include activation of phosphatidylinositol 3-kinase/Akt, and the downstream mediator AS160. Furthermore, Rho-kinase was also involved in the regulation of insulin action.[28] Since HPE improved insulin resistance, it could be implicated in the signal cascades.

Although our diabetes model was induced and based on obesity, it was notable that the diabetic rats lost weight after a few weeks. This phenomenon coincides with a common clinical finding among type 2 diabetic patients, and represents the imbalance of energy expenditure caused by impairment of the insulin function. However, with HPE, the experimental animals regained their weight, implying a recovery of metabolic balance.

In addition to the present study, some previous reports have also suggested the benefits of *H. sabdariffa* for diabetic complications. *H. sabdariffa* lowered TG, cholesterol, LDL cholesterol and apo-B100, while elevating HDL cholesterol in diabetic patients.[29] Consuming *H. sabdariffa* decreased systolic BP in type 2 diabetic patients with mild hypertension.[30] Metabolic syndrome patients treated with *H. sabdariffa* had significantly improved glucose levels and lipid profiles, and also a reduced TAG/HDL-c ratio, a marker of insulin resistance.[31] The ethanolic extract of *H. sabdariffa* possessed strong hypolipidemic and antioxidative properties in alloxan-induced diabetic rats, and therefore could be useful in preventing atherosclerosis or related cardiovascular pathologies associated with diabetes.[32]

Figure 2 and Table 2 show that at least 18 phenolic compounds are found in the composition of HPE. In fact, many polyphenolic components identified in HPE, including gallic acid, protocatechuic acid, chlorogenic acid, caffeic acid, galloyl ester, quercetin derivative, and tiliroside, were reported to be antidiabetic.[33−39] These components exerted an effect on insulin-secretagogue, antihyperglycemia and antiglycation. As a result, they regulated glucose metabolism and prevented diabetic damage to the liver, pancreas, and kidney. HPE is safe to use and did no harm to livers and kidneys (data not shown).

In conclusion, we have demonstrated the anti-insulin resistance properties of HPE, which demonstrated effects on hypoglycemia, hypolipidemia, and antioxidation. HPE has the potential to act as an adjuvant for diabetic therapy, and deserves further investigation.

AUTHOR INFORMATION

Corresponding Author

*C.-J.W.: tel, 866-4-24730022 ext 11670; fax, 866-4-23248167; e-mail, wcj@csmu.edu.tw. C.-N.H.: tel, 866-4-24739595 ext 34711; fax, 866-4-24739220; e-mail, cshy049@csh.org.tw.

Author Contributions

#These authors contributed equally to this work and, therefore, share the corresponding authorship.

Funding Sources

Funding for this research was provided by the National Science Council (NSC), Taiwan, under NSC 97-2320-B-241-003-MY3, and Chung-Shan Medical University Hospital, under CSH 2010-C-005.

ACKNOWLEDGMENT

The authors acknowledge the contributions of Professor Jen-Dong Hsu (Department of Pathology and Clinical Laboratory, Chung Shan Medical University Hospital, Taichung, Taiwan) in histological consultations.

REFERENCES

(1) Despres, J. P. Is visceral obesity the cause of the metabolic syndrome? *Ann. Med.* **2006**, *38*, 52–63.

(2) Wautier, J. L.; Guillausseau, P. J. Advanced glycation end products, their receptors and diabetic angiopathy. *Diabetes Metab.* **2003**, *27*, 535–542.

(3) Forbes, J. M.; Yee, L. T.; Thallas, V.; Lassila, M.; Candido, R.; Jandeleit-Dahm, K. A.; Thomas, M. C.; Burns, W. C.; Deemer, E. K.; Thorpe, S. R.; Cooper, M. E.; Allen, T. J. Advanced glycation end product interventions reduce diabetes-accelerated atherosclerosis. *Diabetes* **2003**, *53*, 1813–1823.

(4) Jedsadayanmata, A.; Chen, C. C.; Kireeva, M. L.; Lau, L. F.; Lam, S. C. Activation-dependent adhesion of human platelets to Cyr61 and Fisp12/mouse connective tissue growth factor is mediated through integrin IIb. *J. Biol. Chem.* **1999**, *274*, 24321–24327.

(5) Lin, H. H.; Huang, H. P.; Huang, C. C.; Chen, J. H.; Wang, C. J. *Hibiscus* polyphenol-rich extract induces apoptosis in human gastric carcinoma cells via p53 phosphorylation and p38 MAPK/ FasL cascade pathway. *Mol. Carcinog.* **2007**, *43*, 86–99.

(6) Lin, T. L.; Lin, H. H.; Chen, C. C.; Lin, M. C.; Chou, M. C.; Wang, C. J. *Hibiscus sabdariffa* extract reduces serum cholesterol in men and women. *Nutr. Res. (N.Y.)* **2007**, *27*, 140–145.

(7) Chen, C. C.; Hsu, J. D.; Wang, S. F.; Chiang, H. C.; Yang, M. Y.; Kao, E. S.; Ho, Y. C.; Wang, C. J. *Hibiscus sabdariffa* extract inhibits the development of atherosclerosis in cholesterol-fed rabbits. *J. Agric. Food Chem.* **2003**, *51*, 5472–5477.

(8) Yang, M. Y.; Peng, C. H.; Chan, K. C.; Yang, Y. S.; Huang, C. N; Wang, C. J. The hypolipidemic effect of *Hibiscus sabdariffa* polyphenols via inhibiting lipogenesis and promoting hepatic lipid clearance. *J. Agric. Food Chem.* **2010**, *58*, 850–859.

(9) Peng, C. H. *Hibiscus sabdariffa* inhibits vascular smooth muscle cell proliferation and migration induced by high glucoses--a mechanism involves connective tissue growth factor signals. *J. Agric. Food Chem.* **2009**, *57*, 3073–3079.

(10) Lee, W. C.; Wang, C. J.; Chen, Y. H.; Hsu, J. D.; Cheng, S. Y.; Chen, H. C.; Lee, H. J. Polyphenol extracts from *Hibiscus sabdariffa* linnaeus attenuate nephropathy in experimental Type 1 Diabetes. *J. Agric. Food Chem.* **2009**, *57*, 2206–2210.

(11) Peng, C. H.; Ker, Y. B.; Weng, C. F.; Peng, C. C.; Huang, C. N.; Lin, L. Y.; Peng, R. Y. Insulin secretagogue bioactivity of Finger Citron Fruit (Citrus medica L. var. Sarcodactylis Hort, Rutaceae). *J. Agric. Food Chem.* **2009**, *57*, 8812–8819.

(12) Taga, M. S.; Miller, E. E.; Pratt, D. E. Chia seeds as a source of natural lipid antioxidants. *J. Am. Oil Chem. Soc.* **1984**, *61*, 928–931.

(13) Jia, Z.; Tang, M.; Wu, J. The determination of flavonoid contents in mulberry and their scavenging effects on superoxide radicals. *Food Chem.* **1999**, *64*, 555–559.

(14) Murphy, M.; Godson, C.; Cannon, S.; Kato, S.; Mackenzie, H. S.; Martin, F.; Brady, H. R. Suppression subtractive hybridization identifies high glucose levels as a stimulus for expression of connective tissue growth factor and other genes in human mesangial cells. *J. Biol. Chem.* **1999**, *274*, 5830–5834.

(15) Li, J.; Liu, N. F.; Wei, Q. Effect of rosiglitazone on cardiac fibroblast proliferation, nitric oxide production and connective tissue growth factor expression induced by advanced glycation end-products. *J. Int. Med. Res.* **2008**, *36*, 329–335.

(16) Ge, Q. M.; Dong, Y.; Su, Q. Effects of glucose and advanced glycation end products on oxidative stress in MIN6 cells. *Cell. Mol. Biol.* **2010**, *56*, 1231–1238.

(17) Steinberg, D.; Parthasarathy, S.; Carew, T. E.; Khoo, J. C.; Witztum, J. L. Beyond cholesterol: Modifications of low-density

lipoprotein that increases its atherogenicity. *N. Engl. J. Med.* **1989**, *320*, 915–919.

(18) Yoon, S. J.; Yoon, Y. W.; Lee, B. K.; Kwon, H. M.; Hwang, K. C.; Kim, M.; Chang, W.; Hong, B. K.; Lee, Y. H.; Park, S. J.; Min, P. K.; Rim, S. J. Potential role of HMG CoA reductase inhibitor on oxidative stress induced by advanced glycation endproducts in vascular smooth muscle cells of diabetic vasculopathy. *Exp. Mol. Med.* **2009**, *41*, 802–811.

(19) Vincent, A. M.; Perrone, L.; Sullivan, K. A.; Backus, C.; Sastry, A. M.; Lastoskie, C.; Feldman, E. L. Receptor for advanced glycation end products activation injures primary sensory neurons via oxidative stress. *Endocrinology* **2007**, *148*, 548–558.

(20) Martinez, J. A. Mitochondrial oxidative stress and inflammation: an slalom to obesity and insulin resistance. *J. Physiol. Biochem.* **2006**, *62*, 303–306.

(21) Berkemeyer, S. The straight line hypothesis elaborated: case reference obesity, an argument for acidosis, oxidative stress, and disease conglomeration? *Med. Hypotheses* **2010**, *75*, 59–64.

(22) Bakker, S. J.; IJzerman, R. G.; Teerlink, T.; Westerhoff, H. V.; Gans, R. O.; Heine, R. J. Cytosolic triglycerides and oxidative stress in central obesity: the missing link between excessive atherosclerosis, endothelial dysfunction, and beta-cell failure? *Atherosclerosis* **2000**, *148*, 17–21.

(23) Mittendorfer, B.; Magkos, F.; Fabbrini, E.; Mohammed, B. S.; Klein, S. Relationship between body fat mass and free fatty acid kinetics in men and women. *Obesity* **2009**, *17*, 1872–1877.

(24) de Jongh, R. T.; Serne, E. H.; Ijzerman, R. G.; de Vries, G.; Stehouwer, C. D. Free fatty acid levelsmodulatemicrovascular function: Relevance for obesity-associated insulin resistance, hypertension, and microangiopathy. *Diabetes* **2004**, *53*, 2873–2882.

(25) Ye, J. Role of insulin in the pathogenesis of free fatty acid-induced insulin resistance in skeletal muscle. *Endocr., Metab. Immune Disord.: Drug Targets* **2007**, *7*, 65–74.

(26) Samuel, V. T.; Petersen, K. F.; Shulman, G. I. Lipid-induced insulin resistance: unravelling the mechanism. *Lancet* **2010**, *375*, 2267–2277.

(27) Bhattacharya, S.; Dey, D.; Roy, S. S. Molecular mechanism of insulin resistance. *J. Biosci.* **2007**, *32*, 405–413.

(28) Choi, K.; Kim, Y. B. Molecular mechanism of insulin resistance in obesity and type 2 diabetes. *Korean J. Intern. Med.* **2010**, *25*, 119–129.

(29) Mozaffari-Khosravi, H.; Jalali-Khanabadi, B. A.; Afkhami-Ardekani, M.; Fatehi, F. Effects of sour tea (*Hibiscus sabdariffa*) on lipid profile and lipoproteins in patients with type II diabetes. *J. Altern. Complementary Med.* **2009**, *15*, 899–903.

(30) Mozaffari-Khosravi, H.; Jalali-Khanabadi, B. A.; Afkhami-Ardekani, M.; Fatehi, F.; Noori-Shadkam, M. The effects of sour tea (*Hibiscus sabdariffa*) on hypertension in patients with type II diabetes. *J. Hum. Hypertens.* **2009**, *23*, 48–54.

(31) Gurrola-Diaz, C. M.; Garcia-Lopez, P. M.; Sanchez-Enriquez, S.; Troyo-Sanroman, R.; Andrade-Gonzalez, I.; Gomez-Leyva, J. F. Effects of Hibiscus sabdariffa extract powder and preventive treatment (diet) on the lipid profiles of patients with metabolic syndrome (MeSy). *Phytomedicine* **2010**, *17*, 500–505.

(32) Farombi, E. O.; Ige, O. O. Hypolipidemic and antioxidant effects of ethanolic extract from dried calyx of *Hibiscus sabdariffa* in alloxan-induced diabetic rats. *Fundam. Clin. Pharmacol.* **2007**, *21*, 601–609.

(33) Hsu, F. L.; Chen, Y. C.; Cheng, J. T. Caffeic acid as active principle from the fruit of xanthium strumarium to lower plasma glucose in diabetic rats. *Planta Med.* **2000**, *66*, 228–230.

(34) Lin, C. Y.; Tsai, S. J.; Huang, C. S.; Yin, M. C. Antiglycative effects of protocatechuic Acid in the kidneys of diabetic mice. *J. Agric. Food Chem.* **2011**, *59*, 5117–5124.

(35) Karthikesan, K.; Pari, L.; Menon, V. P. Combined treatment of tetrahydrocurcumin and chlorogenic acid exerts potential antihyperglycemic effect on streptozotocin-nicotinamide-induced diabetic rats. *Gen. Physiol. Biophys.* **2010**, *29*, 23–30.

(36) Chao, C. Y.; Mong, M. C.; Chan, K. C.; Yin, M. C. Anti-glycative and anti-inflammatory effects of caffeic acid and ellagic acid in kidney of diabetic mice. *Mol. Nutr. Food Res.* **2010**, *54*, 388–395.

(37) Kim, J. H.; Kang, M. J.; Choi, H. N.; Jeong, S. M.; Lee, Y. M.; Kim, J. I. Quercetin attenuates fasting and postprandial hyperglycemia in animal models of diabetes mellitus. *Nutr. Res. Pract.* **2011**, *5*, 107–111.

(38) Park, C. H.; Noh, J. S.; Yamabe, N.; Kang, K. S.; Tanaka, T.; Yokozawa, T. Beneficial effect of 7-O-galloyl-D-sedoheptulose on oxidative stress and hepatic and renal changes in type 2 diabetic db/db mice. *Eur. J. Pharmacol.* **2010**, *640*, 233–242.

(39) Zhu, Y.; Zhang, Y.; Liu, Y.; Chu, H.; Duan, H. Synthesis and biological activity of trans-tiliroside derivatives as potent anti-diabetic agents. *Molecules* **2010**, *15*, 9174–9183.